

## **General Disclaimer**

### **One or more of the Following Statements may affect this Document**

- This document has been reproduced from the best copy furnished by the organizational source. It is being released in the interest of making available as much information as possible.
- This document may contain data, which exceeds the sheet parameters. It was furnished in this condition by the organizational source and is the best copy available.
- This document may contain tone-on-tone or color graphs, charts and/or pictures, which have been reproduced in black and white.
- This document is paginated as submitted by the original source.
- Portions of this document are not fully legible due to the historical nature of some of the material. However, it is the best reproduction available from the original submission.

X-651-71-195  
PREPRINT

NASA TM X- 65560

# NUMERICAL SOLUTION FOR CHEMICALLY GENERATED WAVES IN A DILUTE, ISOTHERMAL ATMOSPHERE

IGOR J. EBERSTEIN  
KENNETH D. SHERE

FACILITY FORM 602	<b>N71-27844</b>	
	(ACCESSION NUMBER)	(THRU)
	<u>25</u>	<u>Q3</u>
	(PAGES)	(CODE)
	<u>TMX-65560</u>	<u>20</u>
	(NASA CR OR TMX OR AD NUMBER)	(CATEGORY)

APRIL 1971

**GSFC**

**GODDARD SPACE FLIGHT CENTER**  
**GREENBELT, MARYLAND**



X-651-71-195

NUMERICAL SOLUTION FOR CHEMICALLY  
GENERATED WAVES IN A DILUTE,  
ISOTHERMAL ATMOSPHERE

Igor J. Eberstein

Kenneth D. Shere

April 1971

GODDARD SPACE FLIGHT CENTER  
Greenbelt, Maryland

# NUMERICAL SOLUTION FOR CHEMICALLY GENERATED WAVES IN A DILUTE, ISOTHERMAL ATMOSPHERE

## I. INTRODUCTION

A study is made of the behavior of chemically generated waves in a simplified atmosphere. The atmosphere is assumed unbounded, isothermal, one-space-dimensional and initially quiescent. At an initial time a dissociation reaction,  $AB + J \rightarrow A + B + J$ , commences and drives the subsequent wave motion. The fraction of reactant in the atmosphere,  $X_0$ , is assumed to be small. The system of governing equations is then expanded in terms of the small parameter,  $X_0$ , and an asymptotic integral solution as  $X_0 \rightarrow 0$  is obtained.

The analytical development is presented in Part 1 (Eberstein and Shere, 1971) and is briefly summarized below.

The non-dimensionalized system of equations was expanded about the parameter  $X_0$ , so that each dependent variable is represented in a series of the form

$$f(t, z) = \sum_{N=0}^{\infty} f^{(N)}(t, z) X_0^N \quad (1.1)$$

where higher order terms may be dropped as  $X_0 \rightarrow 0$ ;  $t$  is a nondimensional time and  $z$  is a nondimensional altitude. Dropping terms of second order and above, one obtains:

$$f(t, z) = f^{(0)} + f^{(1)} X_0 \quad (1.2)$$

Further define subscripted quantities for the density  $\rho$ , fraction of reactant dissociated  $\alpha$  and temperature  $T$  such that



$$f^{(0)} = f_{(0)} \quad (1.3)$$

$$f^{(1)} = f^{(0)} f_{(1)} \quad (1.4)$$

and for the velocity  $u$  such that

$$u^{(1)} = u_{(1)}. \quad (1.5)$$

It follows that

$$f = f^{(0)} (1 + X_0 f_{(1)}). \quad (1.6)$$

In terms of subscripted quantities, the linearized, non-dimensionalized system of equations describing the atmosphere is given below:

$$\frac{\partial \rho_{(1)}}{\partial t} + \frac{\partial u_{(1)}}{\partial z} - u_{(1)} = 0 \quad (1.7)$$

$$\frac{1}{g} \frac{\partial u_{(1)}}{\partial t} + \frac{\partial \rho_{(1)}}{\partial z} - T_{(1)} + \frac{\partial T_{(1)}}{\partial z} = \alpha^{(0)} \quad (1.8)$$

$$-\frac{\partial \rho_{(1)}}{\partial t} + \frac{1}{\gamma - 1} \frac{\partial T_{(1)}}{\partial t} + u_{(1)} = -\mathcal{B} \frac{\partial \alpha_{(0)}}{\partial t} \quad (1.9)$$

$$\alpha^{(0)} = 1 - \exp [-k_F \rho^{(0)} t] \quad (1.10)$$

The above equations are respectively, continuity, momentum, energy, and extent of reaction.

$\mathcal{B}$  is defined as:

$$\mathcal{B} \equiv (B/T_0 - 1) \quad (1.11)$$

where B is the enthalpy of reaction;

$T_0$  is unperturbed temperature;

$\rho_0$  is unperturbed density;

g is gravitational acceleration.

Defining  $\theta = e^{-z/2} T_{(1)}$  and taking the following initial conditions for  $\theta$ :

$$\theta(0, z) = 0$$

$$\theta_t(0, z) = -(\gamma - 1) B k_F \exp(-3z/2) \quad (1.12)$$

$$\theta_{tt}(0, z) = (\gamma - 1) B k_F^2 \exp(-5z/2)$$

One obtains the solution  $\theta = \theta_1 + \theta_2$  where

$$\theta_1(t, z) = [-(\gamma - 1) B k_F / (c \sqrt{2})] (t \exp(-ct \sqrt{2})) \exp(-3z/2) \quad (1.13)$$

and  $\theta_2(t, z)$  satisfies the equation:

$$\frac{\partial^2}{\partial t^2} M[\theta] = f(\alpha) \exp(-z/2) \quad (1.14)$$

with  $M[.]$  the operator

$$M[.] = \frac{\partial^2}{\partial t^2} - c^2 \frac{\partial^2}{\partial z^2} + \frac{c^2}{4} \quad (1.15)$$

Integrating (1.14) with respect to time twice, one obtains

$$M[\theta] = w(t, z) - M[\theta_1]$$

where

$$w(t, z) = -k_F (\gamma - 1) B \Omega_1 \Omega_2,$$

$$\Omega_1 \equiv k_F \left( \frac{1}{T_0} - \frac{1}{B} - t^2 \right) + 2 t e^{+z}, \quad (1.16)$$

$$\Omega_2 \equiv \exp [-(5z/2 + k_F t e^{-z})].$$

Then,  $\theta_2(t, z)$  is given as follows:

$$\theta_2(t, z) = \int_0^t W(t, z, \tau) d\tau. \quad (1.17)$$

Taking  $\zeta = \tau c$ , the expression for  $W$  becomes:

$$W(t, z, \tau) = \int_0^{tc-\zeta} \left[ J_0 \left( \frac{1}{2} \sqrt{(tc-\zeta)^2 - \eta^2} \right) \right] Q(\tau, z, \eta) d\eta \quad (1.18)$$

where

$$Q(\tau, z, \eta) = [w(\tau, z + \eta) + w(\tau, z - \eta)] / 2c^2 \quad (1.19)$$

The first order terms are then:

$$T(t, z) = e^{z/2} \theta(t, z); \quad (1.20)$$

$$u(t, z) = - \int_{z_s}^z \frac{\partial}{\partial t} \left[ \frac{T}{\gamma - 1} + \beta a \right] dz \quad (1.21)$$

where  $z_s$  is at the earth's surface.

Defining

$$E = \frac{T}{\gamma - 1} + \beta a \quad (1.22)$$

and substituting into (1.21) yields:

$$\frac{\partial u}{\partial z} = - \frac{\partial E}{\partial t} \quad (1.23)$$

and

$$\int_0^t \frac{\partial u}{\partial z} dt = - E(t, z)$$

since  $E(0, z) = 0$ .

From the linearized solution we have:

$$\rho(t, z) = \int_0^t \left[ u - \frac{\partial u}{\partial z} \right] dt. \quad (1.24)$$

From (1.21) - (1.23),

$$\int_0^t u dt = - \int_0^t \int_{z_s}^z \frac{\partial E}{\partial t} dz dt. \quad (1.25)$$

Reversing the order of integration one obtains:

$$\int_0^t u dt = - \int_{z_s}^z \int_0^t \frac{\partial E}{\partial t} dt dz = - \int_{z_s}^z E(t, z) dz. \quad (1.26)$$

substituting (1.26) into (1.24) yields the expression:

$$\rho(t, z) = E(t, z) - \int_{z_s}^z E(t, z) dz. \quad (1.27)$$

## II. COMPUTING

The mathematical development of the solution was briefly outlined above. A discussion of numerical procedures is now presented.

The core of the numerical problem is evaluation of the integral expressions

$$\theta_2(t, z) = \int_0^t W(t, z, \tau) d\tau \quad (2.1)$$

and

$$W(t, z, \tau) = \int_0^{tc - \tau c} \left[ J_0 \left( \frac{c}{2} \sqrt{(t - \tau)^2 - \left( \frac{\eta}{c} \right)^2} \right) \right] Q(\tau, z, \eta) d\eta \quad (2.2)$$

Evaluation of the above integrals was done numerically using Euler's method:

$$\theta(t, z) = \sum_{i=0}^N W_i(t, z, \tau_i) \Delta\tau \quad (2.3)$$

where  $\Delta\tau \equiv t/N$  and  $\tau_i \equiv i\Delta\tau$ .

Similarly,

$$W = \sum_{j=0}^M \left[ J_0 \left( \frac{c}{2} \sqrt{(t - \tau_i)^2 - \left( \frac{\eta_j}{c} \right)^2} \right) \right] Q(\tau_i, z, \eta_j) \Delta\eta \quad (2.4)$$

where

$$\Delta\eta \equiv (t - \tau) c/M$$



and

$$\eta_j = j \Delta \eta$$

The Bessel function was evaluated using an integral expression. Accuracy of the routine was checked against tables in the handbook of Chemistry and Physics. Agreement was five significant figures or better.

The size of the integration mesh was decreased until the results became invariant to further decreases of mesh size.

The above procedure works quite well, except for situations where the time becomes very long. If the integration steps are kept small, then computer time becomes long. Conversely, if the number of intervals is kept constant, then accuracy suffers. Also, one would like to observe how the perturbation profile develops with time. It would thus be desirable to break up the integral for  $\theta_2$  into a series of integrals as follows:

$$\theta_2(t, z) = \sum_{k=1}^K \int_{\Delta t(k-1)}^{\Delta tk} W(t_k, z, \tau) d\tau \quad (2.5)$$

where  $K$  is chosen such that

$$t = K \Delta t$$

The above procedure could be followed quite arbitrarily if  $W$  were not a function of final time,  $t$ . At this point it becomes helpful to invoke some physical reasoning.

Let us first examine the expression for  $W$ , i.e.

$$W(t, z, \tau) = \int_0^{tc - \tau c} \left[ J_0 \left( \frac{1}{2} \sqrt{(tc - \tau c)^2 - \eta^2} \right) \right] Q(\tau, z, \eta) d\eta$$

The quantity  $\sqrt{(tc - \tau c)^2 - \eta^2}$  is familiar from the theory of wave propagation.  $(t - \tau)c$  is the distance that a wavelet has travelled in time  $(t - \tau)$ . Thus the  $\eta$  integration goes to  $c(t - \tau)$ , or to the limits of the physical region being considered, provided that there is no reflection at the boundaries.

$$Q(\tau, z, \eta) = [w(\tau, z + \eta) + w(\tau, z - \eta)] / 2c^2$$

where  $w = 0$  outside the reaction zone. Let  $e_{\max}$  be the distance from the furthest point in the region considered to the furthest point in the reaction zone. If  $tc > e_{\max}$ , one has summed all the contributions. Defining  $\Delta t \geq e_{\max}/c$ , it is thus permissible to write:

$$\theta_2 = \int_0^{\Delta t} W d\tau + \int_{\Delta t}^{2\Delta t} W d\tau + \cdots + \int_{(n-1)\Delta t}^{n\Delta t} W d\tau$$

with

$$W = \int_0^{c(k\Delta t - \tau)} J_0 Q d\eta$$

and

$$(k - 1) \Delta t \leq \tau \leq k \Delta t.$$

The quantity  $t - \tau$  ranges from zero to  $\Delta t$  making the values of the Bessel function independent of  $k$ . Since the range of  $\eta$  is thus  $tc$ , it becomes possible to compute a matrix of Bessel functions

$$MJ_0(I, J)$$

where the index I refers to  $(t - \tau)$  (I) and the index J refers to  $\eta$  (J). Q, however, depends on the actual time elapsed, and must thus be computed for each value of k. The integral for W thus becomes

$$W(K, I) = \sum_{J=1}^{JMAX} MJ_0(I, J) Q(K, J) \Delta \eta(J)$$

where

$$\tau = \tau(K)$$

Also,

$$\theta_2 = \sum_{I=1}^{IMAX} \theta_I(I)$$

and

$$\theta_I(I) = \sum_{K=1}^{KMAX} W(K, I) \Delta \tau(K)$$

The rate of change of temperature, or  $\theta$ , is needed to evaluate the velocity. This is computed using the forward difference approximation:

$$\frac{d\theta}{dt} \approx \frac{\Delta \theta}{\Delta t} = \frac{\theta_n - \theta_m}{t_n - t_m}$$

The derivatives of  $\theta_1$  and  $\alpha$  are evaluated from exact analytical expressions. Once the temperature and alpha derivatives have been evaluated, the velocity is estimated by a simple numerical integration in  $Z$ , taking the velocity at the earth's surface to be zero. The accuracy of this integration can be improved by taking a finer mesh of  $Z$ . Once the velocity is known it becomes a simple matter to evaluate the density and pressure deviations.

It should be noted that the step sizes for  $Z$  were between  $0.1 H$  and  $0.5 H$ . Thus the velocity and density estimates are generally less reliable than the temperature estimates.

### III. NUMERICAL RESULTS

At very short times a pulse is seen propagating up and down from the reaction zone. The initial pulse has the appearance of a discontinuity. Eventually the pulse passes outside the range of the computation regime, and a pseudo-steady pattern is established in which the qualitative behavior of the parameters does not change. However, the quantitative values increase to a maximum, then decay. The development and decay of the pseudo-steady patterns may be seen in Figures 1 through 3.

The type of behavior observed may be partially explained by analogy with a shock tube whose driven end is semi-infinite. Initially the shock passes, then a pseudo-steady state is established and eventually decays. The above analogy is incomplete, since the atmosphere also behaves like an elastic medium resulting in the establishment of something like a standing wave pattern. However, an acoustic treatment would be incorrect. Firstly, the gravity restoring force is important,

and secondly, the reaction generates pulses all of one sign, either compression or rarefaction. Perhaps another analogy is a spring with weights at the end. When weights are suddenly added or removed, wave patterns are set up in the spring. Now, consider that a series of weights are added or removed in succession. Also, let the spring be very stiff near the bottom, becoming progressively more elastic toward the top.

But enough analogy. Let us proceed to examine the patterns in Figures 1-4.

Figure 1 shows buildup of the  $\theta$  profile. The reaction zone was chosen to be 0.5 H deep, the reaction was exothermic, and the nondimensional rate constant was 0.01. The reference value,  $\omega_R$ , was  $10^{-2} \text{ sec}^{-1}$ ; thus time is given in units of 100 seconds. The characteristic time of the reaction is defined as the point where  $k_F t = 1$ . Strictly speaking, one needs  $k_F \rho^{(0)} t = 1$ , but  $\rho^{(0)} = 1$  at the bottom of the reaction zone. Since  $\rho^{(0)}$  drops off exponentially with altitude, while  $k_F$  remains constant, it follows that the characteristic time increases exponentially with altitude until the end of the reaction zone is reached. It may be shown that

$$k_F t = k_F^* t^*$$

where the starred quantities are dimensional. For  $k_F^* = 10^{-2} \text{ sec}^{-1}$  the characteristic time is  $10^2$  in non-dimensional units, or  $10^4 \text{ sec} = 2.8 \text{ hrs}$ . At  $z = 0.5 \text{ H}$ , the characteristic time becomes 4.6 hrs.

The maximum value of  $\theta$  is at  $z = 0$  and grows with time. A second maximum is found at  $z = 10$ , this secondary maximum also grows with time. Essentially,  $\theta$  follows a bessel function type of altitude pattern as might be expected. The



rates of growth of  $\theta$  at  $z = 0$  and at  $z = 10$  are shown in Figures 2 and 3. The growth is seen to be almost linear initially, tapering off to a maximum, then decaying. Figure 4 shows development of the temperature profiles.

Outside the reaction zone the velocity equation becomes:

$$\frac{\partial u}{\partial z} = \frac{-1}{\gamma - 1} \frac{\partial T}{\partial t}$$

During the buildup of temperature we have

$$\frac{\partial T}{\partial t} > 0$$

everywhere except in a small region near six scale heights. One may conclude that velocity is generally negative during the buildup phase, especially above 8 scale heights. This conclusion is indeed correct.

Physically we know that subsidence in an isothermal atmosphere results in heating. Conversely, an upward motion gives rise to cooling. This is precisely the kind of behavior observed, so we may conclude that the result is physically consistent. Similarly, convergence of velocity results in compression while divergence gives rarefaction. These combined effects are illustrated in Figure 5 which, incidentally is for an endothermic reaction, five scale heights deep.

If we had an adiabatic lapse rate, then physical argument would lead us to expect disappearance of the most pronounced part of the temperature wave. However, the velocity wave would not disappear; consequently, a temperature effect would become visible at an altitude where the lapse rate became less than adiabatic. If the atmosphere has an inversion, then the temperature wave would be especially pronounced.

Several special cases will now be considered:

The first case to be considered is a severe rain storm. Take saturated air at 5 km altitude (270 degrees Kelvin) and condense 25% of it to ice, using a reaction characteristic time of 3 hours and a reaction depth of half of a scale height. The mixing ratio,  $X_0$  is 0.002, and the non-dimensional enthalpy,  $B$ , is a little less than 200. The reaction is of course exothermic. Since the extent of a rainstorm, or even a hurricane, is not large enough to really warrant a one-dimensional approximation, the storm was assumed to be approximated by a line source centered at 6 H below ground level. The above approximation results in a  $\frac{1}{R}$  amplitude fall-off relative to the pure one dimensional case. It is realized that the two-dimensionality correction employed is quite arbitrary, and that a genuine two-dimensional solution of the atmospheric equations of motion should really be used. However, the results, shown in Figure 4, seem to agree reasonably well with experimental observations, as shown by Eberstein and Theon (1971).

Our calculations were taken to ten scale heights above the bottom of the reaction zone. Whereas ten scale heights was chosen quite arbitrarily, there are nonetheless compelling reasons for limiting the vertical extent to which computations are carried out. Firstly, the one-dimensional assumption becomes ever less meaningful as the vertical extent of space is increased. Secondly, the temperature perturbation involves an exponential in altitude, i.e.,

$$T = \theta e^{Z/2}$$

with the consequence that small errors in  $\theta$  can give rise to large temperature errors as  $Z$  becomes large. Also, the non-dissipation and isothermal atmosphere

assumptions lose validity as one considers effects propagating over large distances. A more detailed and comprehensive theory would be needed to study the effect of severe thunderstorms or hurricanes on regions in the ionosphere and above. But we can say at this point is that such effects would definitely be expected. Such a conclusion is indeed borne out by experimental observations. Thus Bauer (1958) has shown a convincing correlation between hurricane passage and electron concentration in the  $F_2$  layer of the ionosphere. More recently, Davies and Jones (1971) have reported association between ionospheric disturbances in the  $F_2$  region and severe thunderstorms. Davies and Jones believe that the ionosphere is perturbed by infrasonic disturbances generated by mechanical motions of the thunderstorms. However, the above authors do not believe that these disturbances are due to buoyancy oscillations. We would suggest that heat released by the storm induces vertical motion (rising or subsiding, but not rapidly oscillating in time) thus influencing the electron concentration and transmission properties of the  $F_2$  layer.

While the ionosphere is outside our quantitative reach, the ozonosphere is relatively accessible, and will now be discussed.

Reed (1950) suggests qualitative explanations in terms of vertical and horizontal motions for correlations between ozone concentration and weather phenomena. The existence of an ozone-weather relationship is described as well known. Reed specifically considers subsidence at high altitudes as one of the means by which ozone concentration is increased.

Our model predicts that a severe storm will cause considerable subsidence at ozone altitudes.

At the time of computation we had considered the velocity and density information to be of secondary importance. A rather crude Z mesh was thus used to save computer time, with the result that the quantitative velocity profiles must be considered approximate. Nonetheless, we are confident that a severe storm causes large and sustained subsidence at ozone altitudes. It would be very interesting to use a fine vertical mesh computation to obtain a quantitative estimate of the ozone concentration change.

One might also consider what effect changes in the ozone layer might have on the rest of the atmosphere. A reaction having the thermal properties of ozone dissociating to molecular oxygen was considered. The reaction characteristic time was taken to be 20 minutes. This results in a maximum perturbation at approximately 4 hours. The type of perturbation profile attained is shown in Figure 5. A 2 degree Kelvin cooling at the first maximum seems quite reasonable (Krueger, 1971). It is then found that at the second maximum (9 H above the bottom of the reaction zone) the temperature change is 15 degrees. The associated density perturbation is 6%, and vertical velocity is 40 cm/sec at 10 minutes, going to 5 cm/sec at 4 hours. Considering that the second maximum is above 90 km where large atmosphere variation are frequently found, one must conclude that upper atmosphere effects of ozone variations are not very important.

A very different conclusion is reached when it comes to the upper atmosphere effects of aurorae. Insofar as a rather large amount of heat is rapidly released in a small altitude regime, the thermodynamic effect of aurorae is very similar to that of a severe thunderstorm or hurricane. The type of behavior expected is thus generally similar to that shown in Figure 4. If one takes an initial heating

rate of 25 ergs/cm<sup>2</sup>-sec and a reaction characteristic time of 20 minutes, with heating concentrated in half a scale height, then the quantitative deviations are approximately the same as those shown in Figure 4. If the mean heating rate is 25 ergs/cm<sup>2</sup>-sec, then the deviations become twice as large. According to D. Heath (1971) auroral heating rates vary between 10 ergs/cm<sup>2</sup>-sec and 100 ergs/cm<sup>2</sup>-sec with heating concentrated in less than one scale height. Corresponding characteristic times vary between 10 minutes and 100 minutes. Since our solution is linear, it becomes possible to estimate upper atmosphere effects anywhere in this range. The maximum temperature deviation predicted is then in the order of 500 degrees at some 200 km for the case of a mean heating rate of 100 ergs/cm<sup>2</sup>-sec. The actual value of 500 degrees must, of course, be taken with a large grain of salt. However, the theory does predict a large temperature increase well above the main auroral display altitude.

#### IV. CONCLUSIONS

A one-dimensional model for impulsive heat release in the atmosphere has been developed. The theory described is intended as a simple tool to study the effects of impulsive heat release. Such heating, or cooling, is found to cause large disturbances at higher altitudes.

The next important development would be to include a second space dimension. It is recognized that solutions including more than one space dimension do exist. Best known among these are acoustic waves, gravity waves, and tidal waves. However, all three above mentioned waves involve special restricted solutions to the atmospheric equations. Specifically, acoustic and gravity waves have



sinusoidal space and time behavior. Tidal waves have a sinusoidal time behavior and a spatial behavior described in terms of Hough functions. The above theories are quite good for evaluating the long distance propagation of periodic disturbances. However, these theories may not readily be employed to study the short distance effects of impulsive heat releases in the atmosphere. Our one-dimensional theory has been an initial step toward an analytical solution to the problem of impulsive heat releases in the atmosphere. Thunderstorms, hurricanes, chemical reactions, and aurorae have been discussed as important natural sources of impulsive heat release.

## REFERENCES

- Bauer, S. J., "Correlation between Atmospheric and Ionospheric Parameters",  
Geofisica Pura e Applicata, Vol. 40 (1958/II) pp. 235-240.
- Bauer, S. J., "An Apparent Ionospheric Response to the Passage of Hurricanes",  
Journ. Geophysical Research, Vol. 63 (1958) pp. 265-269.
- Davies, K. and Jones, J. E., "Ionospheric Disturbances in the F<sub>2</sub> Region Associated with Severe Thunderstorms", J. Atmos. Sci., Vol. 28 (1971) pp. 254-262.
- Eberstein, I. J. and Shere, K., "A Linearized Approach to Chemically Generated Waves in a Dilute, Isothermal Atmosphere", Goddard X-document X-651-71-71, February 1971.
- Eberstein, I. J. and Theon, J., "Estimated Effect of the Release of Latent Heat in the Troposphere on Vertical Temperature Structure in the Atmosphere" submitted to Journal of Atmospheric Sciences, 1971.
- "Handbook of Chemistry and Physics", 43rd Edition, 1961-62. Chemical Rubber Publishing Co., Cleveland, Ohio.
- Heath, D. Personal Communication, Goddard Space Flight Center, Jan. 1971.
- Krueger, A. Personal Communication, Goddard Space Flight Center, April 1971.
- Reed, R. J., "The Role of Vertical Motions in Ozone-Weather Relationships", J. of Meteorology, Vol. 7, pp. 263-267, (1950).

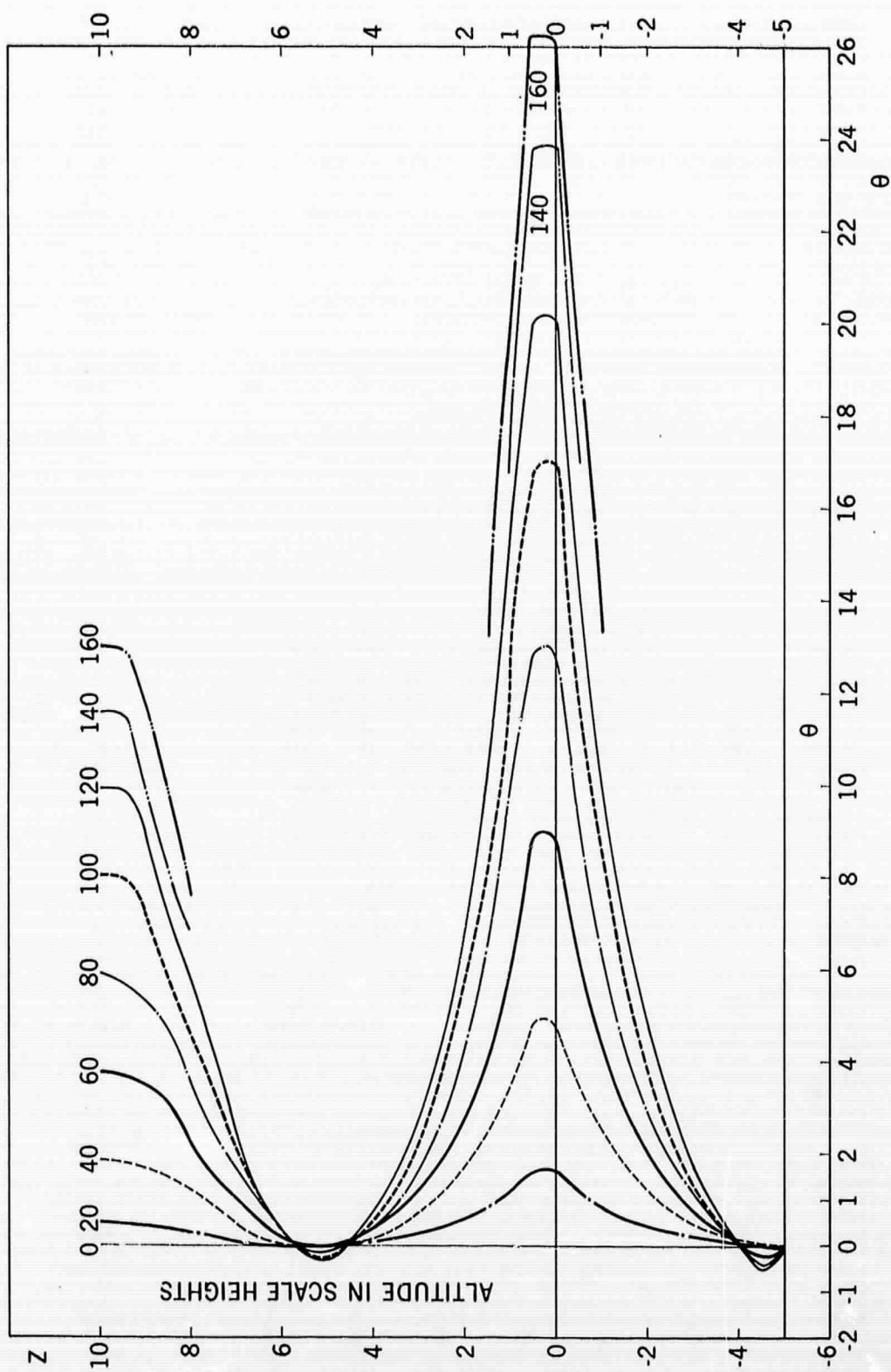


Figure 1.  $\theta$  Profiles

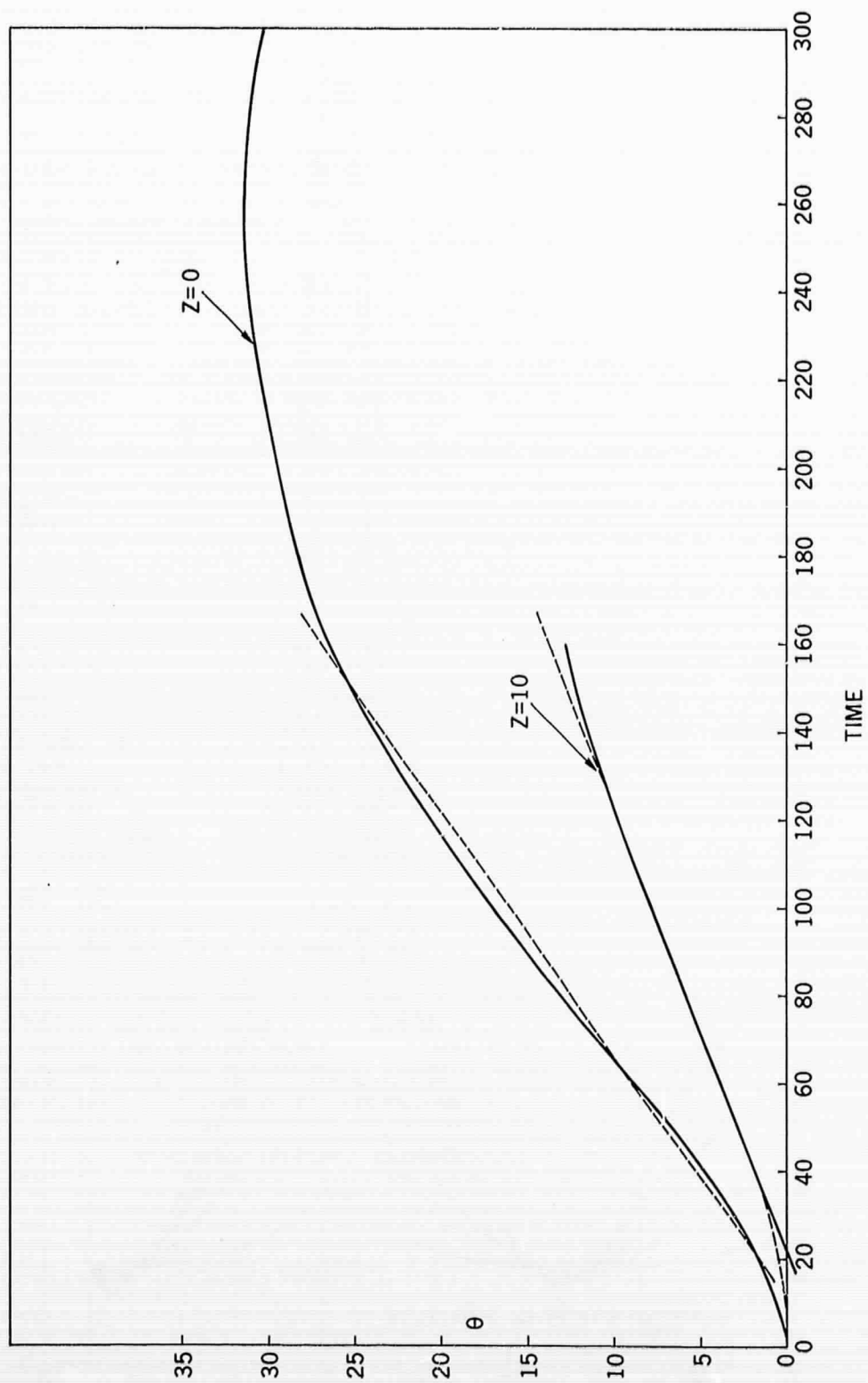


Figure 2.  $\theta$  Development with Time at  $z = 0$  and at  $z = 10$

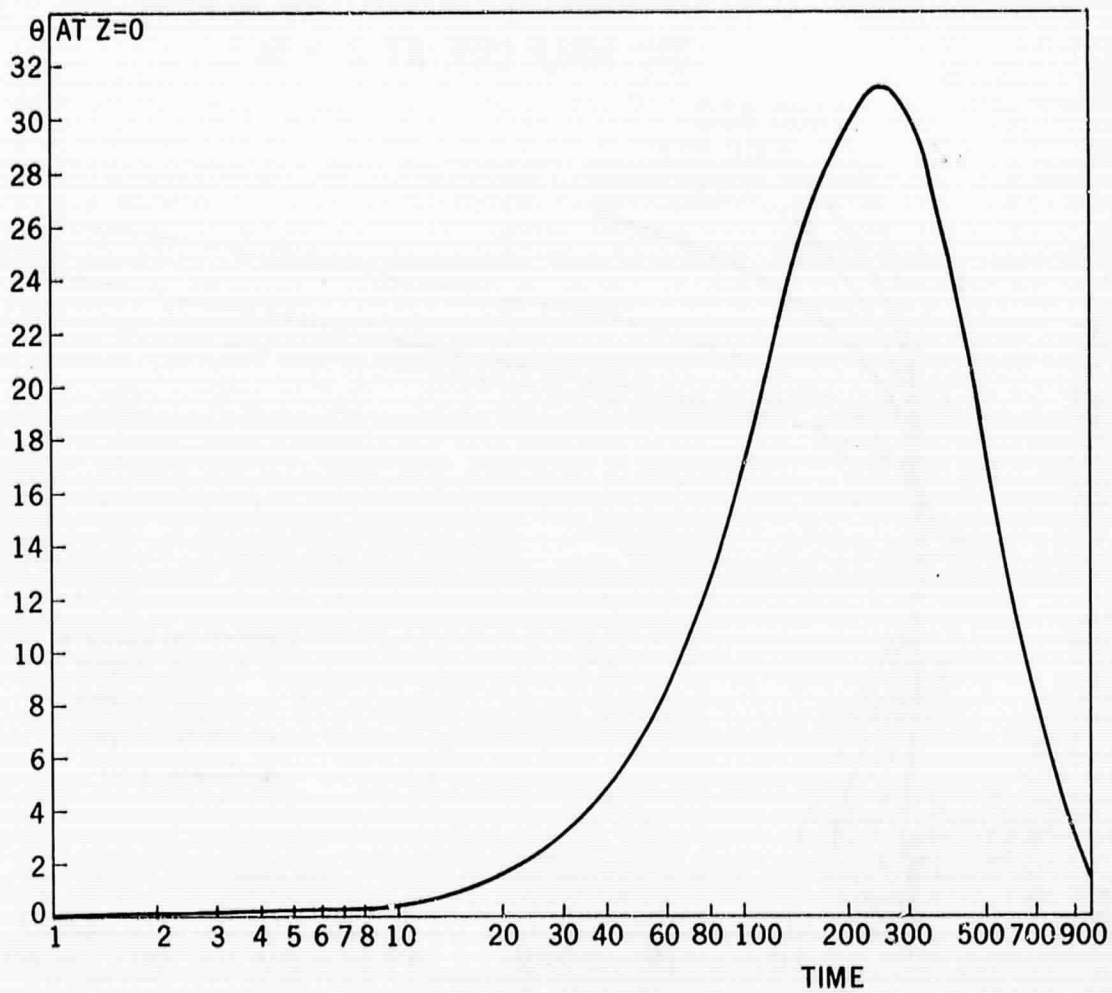


Figure 3.  $\theta$  Development with Time at  $z = 0$



# TEMPERATURE DEVIATION FOR STORM 3hr HALF-LIFE AT $Z = 14$

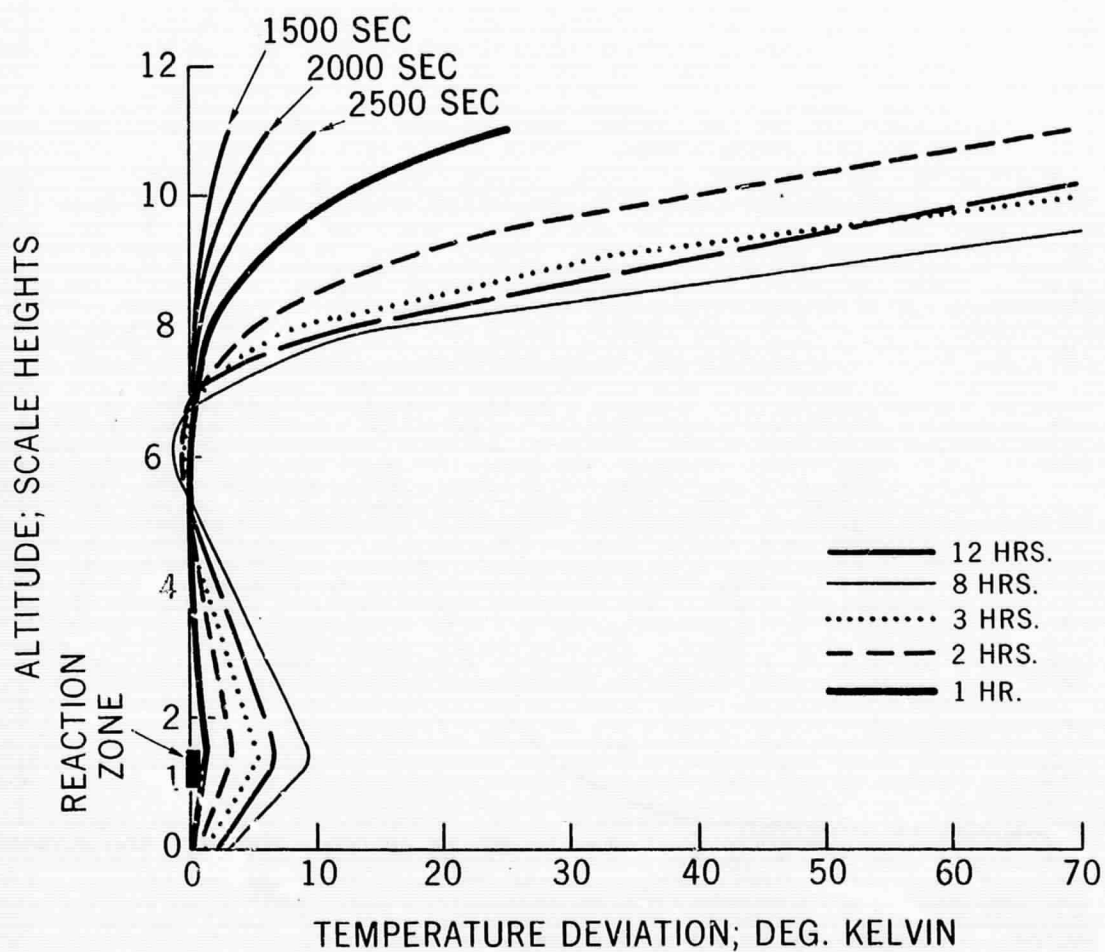


Figure 4. Temperature Deviation for Storm

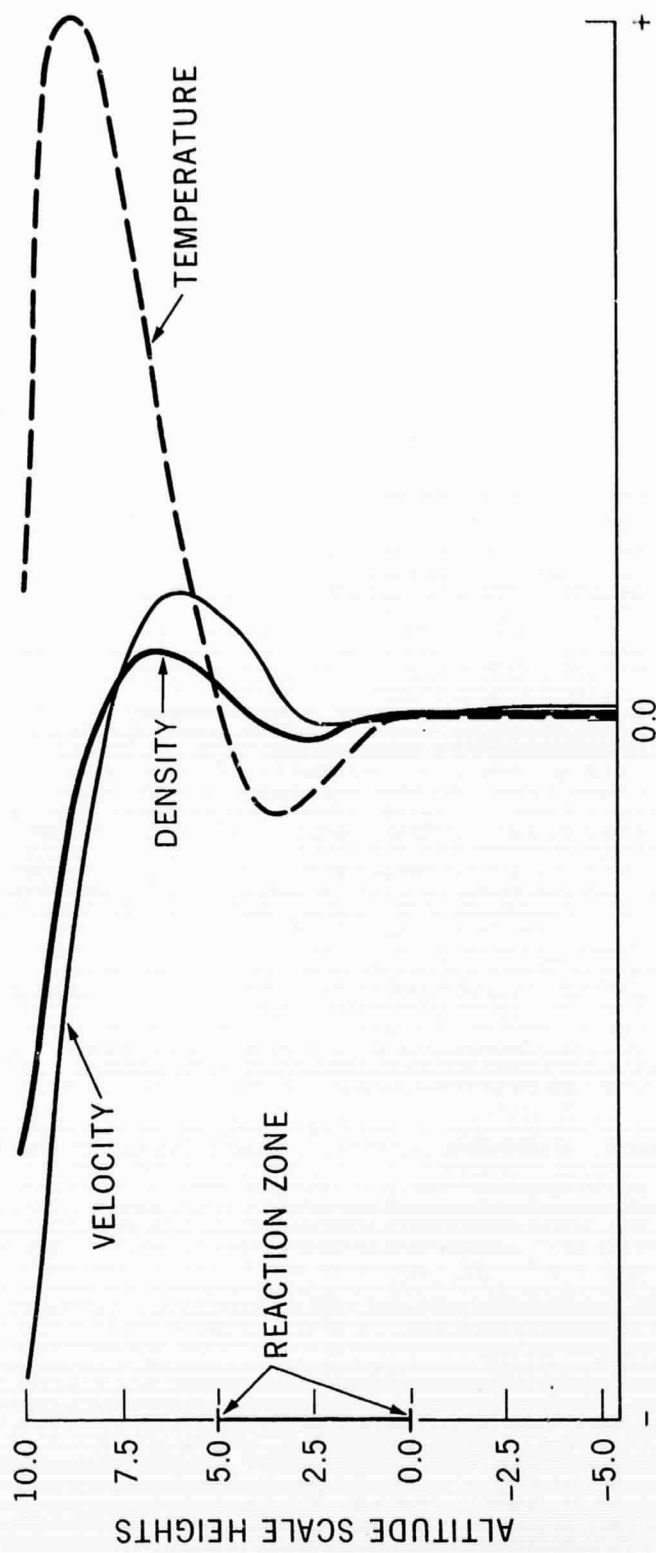


Figure 5. Profiles of Perturbation Temperature, Velocity and Density